

# The role of protecting groups in the formation of organogels through a nano-fibrillar network formed by self-assembling terminally protected tripeptides

Apurba K. Das,<sup>a</sup> Partha Pratim Bose,<sup>a</sup> Michael G. B. Drew<sup>c</sup> and Arindam Banerjee<sup>a,b,\*</sup>

<sup>a</sup>Department of Biological Chemistry, Indian Association for the Cultivation of Science, Jadavpur, Kolkata 700 032, India

<sup>b</sup>Chemistry Division, Indian Institute of Chemical Biology, Jadavpur, Kolkata 700032, India

<sup>c</sup>School of Chemistry, The University of Reading, Whiteknights, Reading RG6 6AD, UK

Received 24 November 2006; revised 5 April 2007; accepted 4 May 2007

Available online 17 May 2007

**Abstract**—A series of eight synthetic self-assembling terminally blocked tripeptides have been studied for gelation. Some of them form gels in various aromatic solvents including benzene, toluene, xylene, and chlorobenzene. It has been found that the protecting groups play an important role in the formation of organogels. It has been observed that, if the C-terminal has been changed from methyl ester to ethyl ester the gelation property does not change significantly (keeping the N-terminal protecting group same), while the change of the protecting group from ethyl ester to isopropyl ester completely abolishes the gelation property. Similarly, keeping the identical C-terminal protecting group (methyl ester) the results of the gelation study indicate that the substitution of N-terminal protection Boc- (*tert*-butyloxycarbonyl) to Cbz- (benzyloxycarbonyl) does change the gelation property insignificantly, while the change from Boc- to pivaloyl (Piv-) or acetyl (Ac-) group completely eliminates the gelation property. Morphological studies of the dried gels of two of the peptides indicate the presence of an entangled nano-fibrillar network that might be responsible for gelation. FTIR studies of the gels demonstrate that an intermolecular hydrogen bonding network is formed during gelation. Results of X-ray powder diffraction studies for these gelator peptides in different states (dried gels, gel, and bulk solids) reflected that the structure in the wet gel is distinctly different from the dried gel and solid state structures. Single crystal X-ray diffraction studies of a non-gelator peptide, which is structurally similar to the gelator molecules reveal that the peptide forms an antiparallel  $\beta$ -sheet structure in crystals.

© 2007 Elsevier Ltd. All rights reserved.

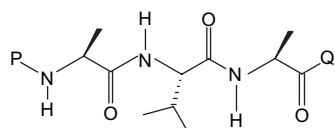
## 1. Introduction

Low molecular weight organogelators have attracted a lot of attention among scientific researchers for the last 15 years.<sup>1</sup> Organogels derived from low molecular mass organic compounds fall into the category of a distinct class of soft materials in which three-dimensional entangled networks are generally formed by various micro-structures or nanostructures including nanofibers,<sup>2</sup> nanotapes,<sup>3</sup> nanoribbons,<sup>4</sup> nanotubes,<sup>5</sup> and these nanostructures being formed through self-assembling gelator molecules using various non-covalent interactions (*viz.* hydrogen bonding, C–H $\cdots\pi$ , N–H $\cdots\pi$ ,  $\pi\cdots\pi$  interactions, metal ion coordination, donor–acceptor interaction, van der Waals' interactions, etc.). The gel-forming network structure can trap a large volume of solvent molecules under appropriate conditions. Self-assembling organogelators have many potential applications as nanostructure

directing agents<sup>6</sup> and as functional materials.<sup>7</sup> There are numerous examples of inorganic hollow nanofibers, which have been prepared efficiently using sol–gel polymerization of various inorganic (Si, V, Ti, etc.) alkoxides in organic solvents containing low molecular mass gelator molecules followed by calcination.<sup>8</sup> Hamachi et al. demonstrated that non-ionic glycosylated amino acid derivatives efficiently gelate a broad spectrum of organic solvents.<sup>9</sup> Tuning of gelation properties has been observed by performing small structural changes in the sugar part of glycosylated amino acid derivatives. Hamilton and Wang reported a series of amino acid-based bis-urea derivatives, which are efficient organogelators.<sup>10</sup> Mono-urea serine derivatives containing an alkyl chain of variable length form gels in water<sup>11</sup> and their gelation properties can be regulated by using minor structural changes at the alkyl chain or at the serine derivatives. Peptide gelators belong to a distinct class of hydrogen bonding gelators in which the gelator molecules self-assemble mainly through intermolecular hydrogen bonding to form the gel network structure. Peptide gels can be treated as an important class of biomaterials as they are made up of naturally occurring amino acid residues. Hydrogels

**Keywords:** Organogelator; Nano-fibrillar; Self-assembly; Synthetic peptide.

\* Corresponding author. Tel.: +91 33 2473 4971; fax: +91 33 2473 5197; e-mail addresses: [bcab@mahendra.iacs.res.in](mailto:bcab@mahendra.iacs.res.in); [arindam@iicb.res.in](mailto:arindam@iicb.res.in)

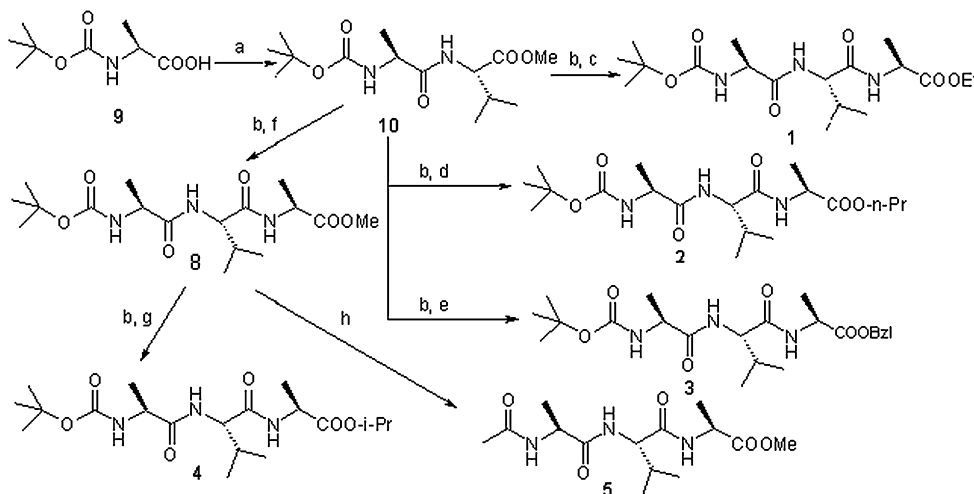


- Peptide 1: P = (CH<sub>3</sub>)<sub>3</sub>C-O(C=O); Q = OCH<sub>2</sub>CH<sub>3</sub>  
 Peptide 2: P = (CH<sub>3</sub>)<sub>3</sub>C-O(C=O); Q = OCH<sub>2</sub>CH<sub>2</sub>CH<sub>3</sub>  
 Peptide 3: P = (CH<sub>3</sub>)<sub>3</sub>C-O(C=O); Q = OCH<sub>2</sub>Ph  
 Peptide 4: P = (CH<sub>3</sub>)<sub>3</sub>C-O(C=O); Q = OCH(CH<sub>3</sub>)<sub>2</sub>  
 Peptide 5: P = CH<sub>3</sub>(C=O); Q = OCH<sub>3</sub>  
 Peptide 6: P = (CH<sub>3</sub>)<sub>3</sub>C(C=O); Q = OCH<sub>3</sub>  
 Peptide 7: P = PhCH<sub>2</sub>-O(C=O); Q = OCH<sub>3</sub>  
 Peptide 8: P = (CH<sub>3</sub>)<sub>3</sub>C-O(C=O); Q = OCH<sub>3</sub>

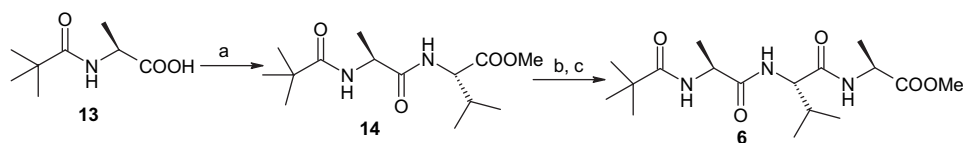
Figure 1. Chemical structures of peptides 1–8.

obtained from self-assembling oligopeptides can be used in tissue repair and engineering.<sup>12</sup> There are several examples of short peptide based hydrogelators.<sup>13</sup> However, there are only a few examples of low molecular weight acyclic peptide based organogelators.<sup>14,15</sup> Until, recently there has been no systematic study investigating the role of protecting groups in organogel formation involving self-assembling synthetic oligopeptides.

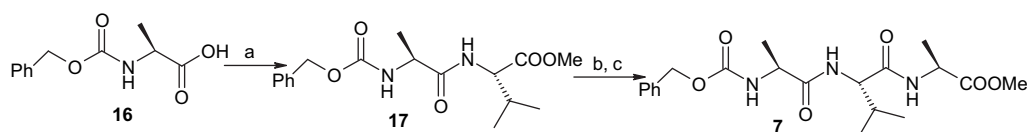
In our previous study, we have reported that low molecular weight synthetic peptides containing non-coded amino acids exhibit supramolecular double columnar sheet-like crystal structures and form thermo-reversible gels in various organic solvents.<sup>14b</sup> In our recent study, we have observed that a terminally protected synthetic tripeptide (containing only proteinaceous amino acids) Boc–Ala–Val–Ala–OMe (peptide 8) forms thermo-reversible gels in various aromatic organic solvents including benzene, toluene, 1,2-dichlorobenzene (*o*-DCB), and xylenes.<sup>15</sup> In this study, we investigate the change/disruption in gelation behavior by modulating the structure of the end groups and thus probing the role of protecting groups in the formation of organogels while keeping the same peptide backbone with the same amino acid sequence. We have therefore synthesized a series of peptides using various protecting groups P–Ala–Val–Ala–Q 1–7 (where P=Boc/Piv/Cbz/Ac and Q=methyl ester/ethyl ester/*n*-propyl ester/isopropyl ester/benzyl ester) (Fig. 1, Schemes 1–3). Results of gelation studies and tuning/abolition of gel-forming tendencies for these molecules are presented here. The way in which precise structural changes in the protecting group alter the gelation properties of the peptides has also been addressed in this paper.



Scheme 1. Reagents and conditions: (a) DMF, H–L–Val–OMe, DCC, HOBT, 0 °C, 83% yield; (b) MeOH, 2 M NaOH, 87.5% yield; (c) DMF, H–L–Ala–OEt, DCC, HOBT, 0 °C, 80% yield; (d) DMF, H–L–Ala–O–*n*-Pr, DCC, HOBT, 0 °C, 76% yield; (e) DMF, H–L–Ala–OBz, DCC, HOBT, 0 °C, 82% yield; (f) DMF, H–L–Ala–OMe, DCC, HOBT, 0 °C, 80% yield; (g) DMF, isopropanol, DCC, HOBT, 0 °C, 80% yield; (h) TFA, acetic anhydride, Et<sub>3</sub>N, 70% yield.



Scheme 2. Reagents and conditions: (a) DMF, H–L–Val–OMe, DCC, HOBT, 0 °C, 80% yield; (b) MeOH, 2 M NaOH, 85% yield; (c) DMF, H–L–Ala–OMe, DCC, HOBT, 0 °C, 82% yield.



Scheme 3. Reagents and conditions: (a) DMF, H–L–Val–OMe, DCC, HOBT, 0 °C, 83% yield; (b) MeOH, 2 M NaOH, 85% yield; (c) DMF, H–L–Ala–OMe, DCC, HOBT, 0 °C, 86% yield.

## 2. Results and discussion

The tripeptides **1**, **2**, **3**, and **7** are readily soluble in different organic solvents on increasing the temperature and when the solutions were allowed to cool to room temperature slowly, translucent gels are obtained within a few minutes. The gelating propensity of these reported tripeptides in a wide range of organic solvents including toluene, benzene, *ortho*-dichlorobenzene (*o*-DCB), *m*-xylene, tetralin, nitrobenzene, and chlorobenzene was studied by dissolving a small amount (1–10% w/v) of compound in 1 mL of the desired solvent under heating. Upon cooling to 30 °C, the complete volume of the respective solvent was immobilized and a gel was formed. The gelation was confirmed by the inverted test tube method. The results of gelation studies in various solvents are summarized in Table 1. These gels are stable toward shaking and they are also stable for a few weeks at room temperature (30 °C). Peptides **1/7** and **8** produce gels in solvents like chlorobenzene, *o*-DCB, toluene, tetralin, and nitrobenzene. Peptide **1** forms a gel in benzene whereas peptide **7** forms a gel in *m*-xylene. Peptide **8** also forms gels in benzene as well as in *m*-xylene. Peptide **1** forms gel more efficiently than peptide **7** in *o*-DCB and nitrobenzene while peptide **7** forms gel more efficiently in toluene than peptide **1**. The efficiency of gelation has been obtained from the minimum gelation concentration (% w/v) of a gelator molecule in a particular solvent. Peptide **2** forms a gel only in *o*-DCB. In chlorobenzene, peptides **1**, **3**, and **7** form gels. Recently, we have observed that the peptide Boc-Ala-Val-Ala-OMe (peptide **8**) produces gels in different aromatic organic solvents including benzene, toluene, *m*-xylene, and *o*-DCB.<sup>15</sup> When we change the C-terminal protecting group from methyl (peptide **8**) to ethyl (peptide **1**) (keeping the N-terminal protecting group same), there is no drastic change in the gelation properties. Table 1 clearly demonstrates that peptide **8** is a more efficient gelator than peptide **1** in aromatic solvents including benzene, toluene, and *o*-DCB. However, this peptide is a less efficient gelator than peptide **1** for gelling organic solvents like tetralin, nitrobenzene, and chlorobenzene. It also forms gel in *m*-xylene whereas peptide **1** fails to form gel in *m*-xylene. It is interesting to notice that when we change the C-terminal protecting group from methyl ester (peptide **8**)/ethyl ester (peptide **1**) to *n*-propyl ester (peptide **2**) to isopropyl ester (peptide **4**) (keeping the N-terminal protecting group intact, i.e. Boc) the gelation property totally vanishes in the case of peptide **4**, while peptide **2** only forms a gel in *o*-DCB at higher concentration. A close inspection of Table 1 also reveals that the peptide **1** is

a more efficient gelator than its structurally similar analog, peptide **3**. Substitution of the N-terminal *tert*-butoxycarbonyl (Boc) group (peptide **1**) by a pivaloyl (in peptide **6**) or by an acetyl (in peptide **5**) group maintaining the C-terminal protecting group, as methyl ester, results in complete removal of gelation properties in peptides **5** and **6**. However, peptide **7** (in which the N-terminal protecting group is benzyloxycarbonyl) forms gels in various aromatic organic solvents including *o*-DCB, toluene, *m*-xylene, chlorobenzene, nitrobenzene and tetralin. It is interesting to note that substitution of the N-terminal Boc group (*tert*-butoxycarbonyl) by Piv (*tert*-butylcarbonyl), which contains one less oxygen atom, completely eliminates the gelation property; while, replacement of the *tert*-butoxycarbonyl group by benzyloxycarbonyl group (in peptide **7**) restores the gelation property.

Thermal stabilities of the peptide gels were analyzed by the dropping ball method.<sup>16</sup> The thermal stabilities of these gels increased upon increasing the concentration of the gelator peptides. In this study, peptides **1** and **7** follow the similar trend wherein the melting temperatures of the peptide gel were found to increase with increasing gelator concentration. The sol–gel phase transition temperatures ( $T_{\text{gel}}$ ) of peptide **1** in *o*-DCB and peptide **7** in toluene are plotted against the gelation concentration in Figure 2. A higher concentration of peptide gelator in the organogels, it is expected that a larger number of molecules are accommodated in the

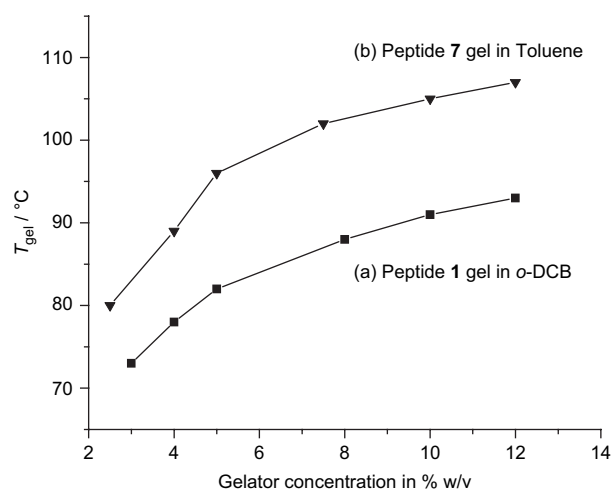


**Figure 2.** The change of  $T_{\text{gel}}$  with respect to gelation concentration of (a) the tripeptide **1** gel in *o*-DCB and (b) the tripeptide **7** gel in toluene.

**Table 1.** Gelation properties of peptides **1–8** in organic solvents<sup>a</sup>

Solvent	<b>1</b>	<b>2</b>	<b>3</b>	<b>4</b>	<b>5</b>	<b>6</b>	<b>7</b>	<b>8</b>
<i>o</i> -DCB	G (3)	G (10)	S	S	S	P	G (5)	G (2.5)
Toluene	G (6)	P	P	S	S	P	G (2.5)	G (5.5)
Benzene	G (10)	S	P	I	I	S	P	G (1.5)
<i>m</i> -Xylene	P	P	P	S	S	P	G (5)	G (7)
Tetralin	G (5)	P	S	P	S	P	G (5)	G (7.5)
Nitrobenzene	G (3)	S	S	S	P	S	G (5)	G (8)
Chlorobenzene	G (5)	S	G (7)	S	S	P	G (5)	G (6)
Cyclohexane	I	P	I	I	P	I	I	I
<i>n</i> -Heptane	I	I	I	I	I	I	I	I
<i>n</i> -Decane	I	P	P	I	P	I	I	I

<sup>a</sup> G: stable gel formed at room temperature; in parentheses: minimum gelation concentration (% w/v); S: soluble; I: insoluble; P: precipitate.

aggregate, because the packing of gelator molecules becomes more pronounced due to enhanced hydrogen bonding interactions, van der Waals' interactions, and other non-covalent interactions.

Transmission electron microscopic (TEM) studies of the dried gels were performed to examine their morphologies. The TEM images of the xerogel obtained from peptide **1** in nitrobenzene (3% w/v) and peptide **7** in toluene (2.5% w/v) show entangled nano-fibrillar networks (Fig. 3a and b, respectively). The fibrillar diameter for the peptide **1** gel varies from 90 to 130 nm, while the width of the fibers in peptide **7** gel is within the range of 50–85 nm. Figure 3(a) represents an entangled nano-fibrillar network while the Figure 3(b) represents the three-dimensional nanotape like structure.

The FTIR spectra of peptide **7** in (a) the solid state, (b) solvent subtracted spectrum in peptide **7**/toluene gel, and (c) dried gel from toluene are presented in Figure 4. The FTIR spectrum of peptide **7**/toluene gel shows absorption bands at 3289 and 1637  $\text{cm}^{-1}$ , which can be assigned as N–H and C=O stretching vibrations. The 3289  $\text{cm}^{-1}$  band is identified as a hydrogen-bonded NH stretching vibration indicating the presence of intermolecular H bonding in the dried gel. The C=O stretching band at 1637–1640  $\text{cm}^{-1}$  (amide I) suggests a  $\beta$ -sheet conformation<sup>17</sup> for peptide **7** in three different states (gel state, dried gel state, and in solid state) indicating little change between these three states. For all reported tripeptide gelators, the FTIR spectra in the solid state as well as in the gel state have been recorded. Each of the reported peptides showed absorption bands at 3270–3375  $\text{cm}^{-1}$  region (N–H stretching vibrations) and 1632–1646  $\text{cm}^{-1}$  region (C=O stretching vibrations). From the solid state and gel state FTIR data it has been suggested that all the reported peptides form intermolecularly hydrogen-bonded  $\beta$ -sheet structures in the solid state as well as in the gel state. However, it is evident from the FTIR data that there is close similarity between the solid state and dried gel state structures, but that they are distinctly different from the wet gel state structure. There is a significant shift (7  $\text{cm}^{-1}$ ) from 3289 to 3296  $\text{cm}^{-1}$  of the N–H stretching vibration in the peptide **7**/toluene gel (wet) state

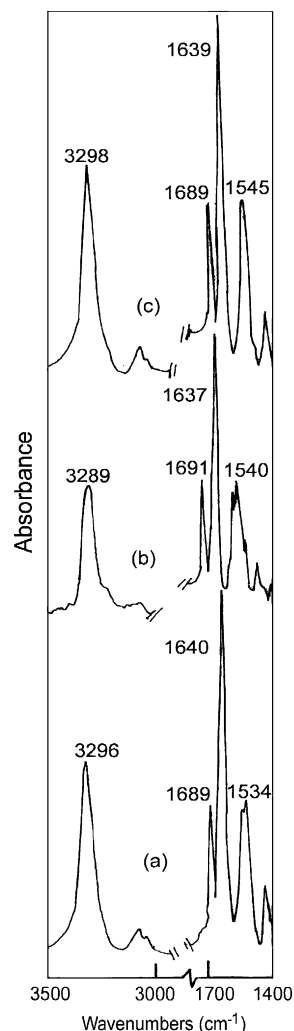


**Figure 4.** FTIR spectra of peptide **7** in (a) solid state, (b) solvent subtracted gel in toluene, and (c) dried gel from toluene.

structure from that of the solid state and 9  $\text{cm}^{-1}$  from 3289 to 3298  $\text{cm}^{-1}$  of the N–H stretching vibration in the peptide **7**/toluene gel (wet) state structure from that of the dried gel state (Fig. 4).

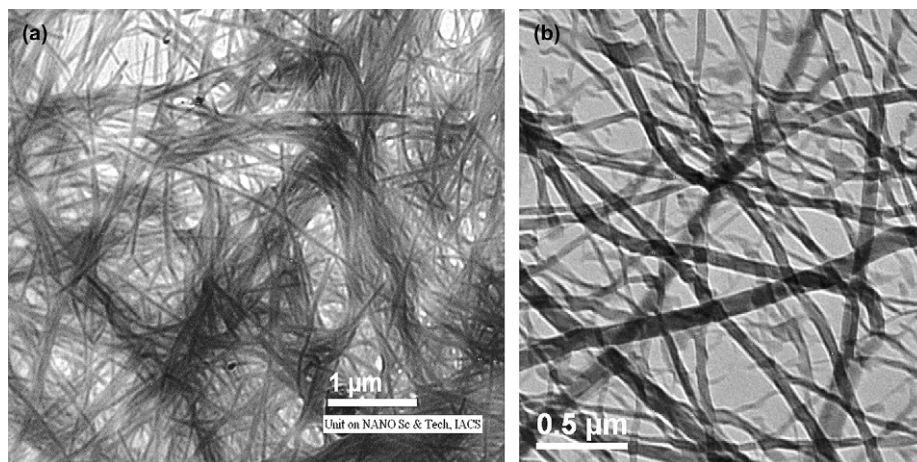


**Figure 3.** Transmission electron micrographs of the dried gel derived from (a) peptide **1** in nitrobenzene (in 3% w/v) and (b) peptide **7** in toluene (in 2.5% w/v).



The molecular packing of the gelator peptides **1**, **3**, and **7** was studied by wide angle X-ray powder diffraction. The major peaks observed are summarized in Table 2. A representative WAXS pattern of the bulk solid of peptide **1**, dried gel obtained from peptide **1**/toluene (5% w/v), and the gel (wet) of peptide **1**/toluene system (5% w/v) is shown in Figure 5. Figure 6 shows the WAXS patterns of bulk solid of peptide **3**, dried gel obtained from peptide **3**/chlorobenzene (10% w/v), and the gel (wet) of peptide **3**/chlorobenzene (10% w/v). Figure 7 also exhibits the representative WAXS patterns of bulk solid of peptide **7**, the dried gel obtained from peptide **7**/toluene (5 wt %), and the wet gel of peptide **7**/toluene system (5 wt %). From Figures 6 and 7, it is clear that the wet gel diffraction patterns show few distinct peaks and this may be due to the heavy scattering of the solvent molecules. Figure 8 exhibits the representative WAXS patterns of non-gelling peptide **6**. For all these cases, distinct interchain distances 3–5 Å were observed. These figures confirm that the fiber responsible for gel formation is a different morph from the bulk solid or the dried gel. The distinct interchain distances 3–5 Å represent the packing observed in non-gelling peptide **6** can be similar with the organization in gel fiber for peptide **1**/toluene gel, peptide **3**/chlorobenzene gel, and peptide **7**/toluene gel. The distinct interchain distance 3–5 Å represents that peptide molecules are intermolecularly hydrogen bonded, which has been confirmed by single crystal X-ray diffraction studies for non-gelator peptide **6**.

In spite of many attempts, we failed to get good quality crystals of gelator molecules. However, we were able to get good quality single crystals of peptide **6**, which is a structurally similar analog of the gelator peptide **1**, although it does not form gels. Crystals were obtained from methanol/water solution by slow evaporation and the crystal has been subjected to a single crystal X-ray diffraction study. In the crystal, tripeptide **6** Piv-Ala(1)-Val(2)-Ala(3)-OMe adopts an overall extended backbone molecular structure in the asymmetric unit. There are two molecules (designated as A and B) in the asymmetric unit for the peptide **6** (Fig. 9). The majority of the backbone torsional angles (except  $\psi_3$  of molecule B) of both molecules A and B for the tripeptide **6** falls within the extended  $\beta$ -sheet region of the Ramachandran diagram.<sup>18</sup> The backbone torsion angles for tripeptide **6** are listed in Table 3. Each conformer (A and B) of the peptide **6** self-assembles via intermolecular hydrogen bonds and other non-covalent interactions to form an infinite supramolecular antiparallel  $\beta$ -sheet assemblage in the crystal along the *b* axis. In tripeptide **6** there are six intermolecular

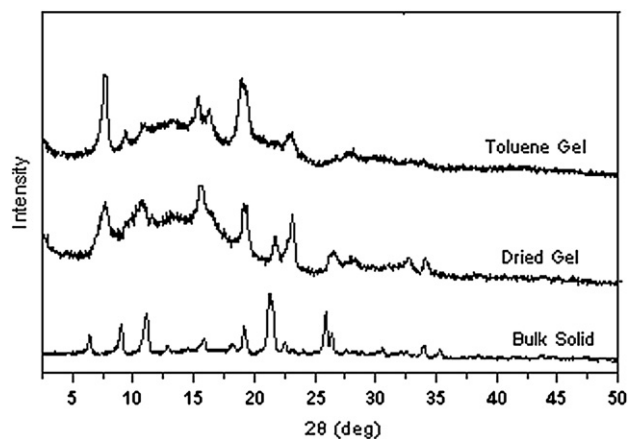


Figure 5. X-ray powder diffraction patterns of peptide **1** under various conditions.

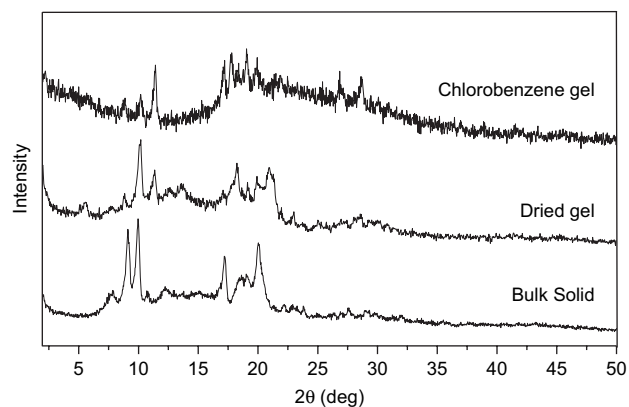


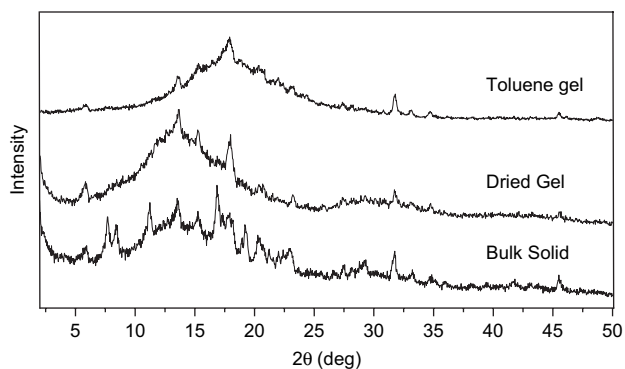
Figure 6. X-ray powder diffraction patterns of peptide **3** under various conditions.

hydrogen bonds (N2A–H2A···O7B, N8A–H8A···O1B, N5A–H5A···O4B, N2B–H2B···O7A, N8B–H8B···O1A, and N5B–H5B···O41A), which stabilize the antiparallel supramolecular monolayer  $\beta$ -sheet structures (Fig. 10). Figure 10 exhibits all hydrogen bonds that are formed between the peptide functionalities. The hydrogen bonding parameters of peptide **6** are listed in Table 4.

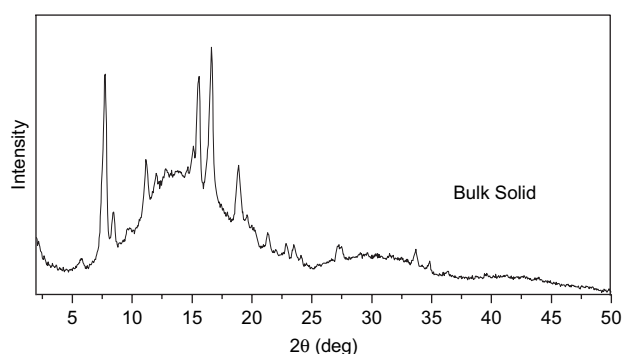
In higher order self-assembly, peptide **6** exhibits a complex quaternary sheet structure by regular stacking of individual peptide molecules via van der Waals interactions and other

Table 2. Major peaks in the XRD pattern for peptides **1**, **3**, and **7** in various conditions

Peptide	<i>d</i> -Spacing [Å]
<b>1</b>	Bulk solid: 11.71, 9.52, 6.71, 5.81, 5.49, 4.7, 3.9, 3.18, 3.03
	Toluene gel: 13.67, 9.75, 6.85, 5.57, 4.85, 4.61, 3.94, 3.43, 3.36, 3.23
	Dried gel: 11.92, 8.56, 5.78, 4.69, 4.14, 3.89, 3.39, 3.22
<b>3</b>	Bulk solid: 11.23, 9.69, 8.87, 8.26, 7.18, 5.15, 4.66, 4.42, 4, 3.87, 3.73, 3.38, 3.23
	Chlorobenzene gel: 10.00, 8.68, 7.76, 5.17, 4.98, 4.65, 4.46, 4.06, 3.31, 3.11
	Dried gel: 15.76, 9.98, 8.67, 7.76, 6.5, 4.85, 4.63, 4.23, 3.86, 3.54, 3.11
<b>6</b>	Bulk solid: 15.38, 11.46, 10.48, 7.91, 7.36, 5.7, 5.33, 4.69, 4.52, 4.15, 3.88, 3.77, 3.26
	Dried gel: 8.44, 6.49, 5.81, 4.94, 4.36, 3.83, 3.05
<b>7</b>	Bulk solid: 15, 11.49, 10.47, 7.87, 6.5, 5.79, 5.25, 5.12, 4.95, 4.68, 4.61, 4.37, 4.18, 4.03, 3.87, 3.6, 3.34, 3.24, 3.05
	Toluene gel: 7.97, 6.52, 4.97, 3.25
	Dried gel: 8.44, 6.49, 5.81, 4.94, 4.36, 3.83, 3.05



**Figure 7.** X-ray powder diffraction patterns of peptide 7 under various conditions.



**Figure 8.** X-ray powder diffraction pattern of peptide 6 (bulk solid).

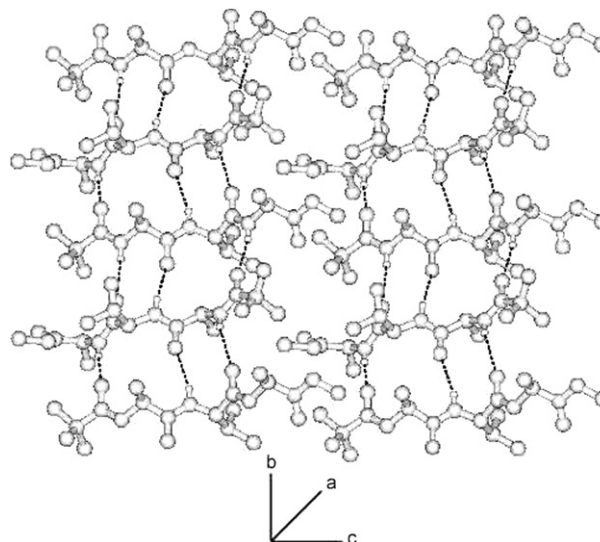
non-covalent interactions along the screw axis parallel to *c* (Fig. 11). From the single crystal X-ray structure analysis of the non-gelator peptide **6**, it is clear that a strong self-complementary and unidirectional intermolecular hydrogen-bonded one-dimensional self-association exists in the primary unit of the crystal of the non-gelator molecules. The crystal structure of a non-gelator molecule, which is

**Table 3.** Intermolecular hydrogen bonds for peptide **6**

Symmetry element	Donor	Acceptor	H...O (Å)	N...O (Å)	N–H...O (°)
—	N2A	O7B	2.36	3.124	148
<sup>a</sup>	N2B	O7A	2.26	3.115	174
<sup>b</sup>	N5A	O4B	2.21	3.060	172
—	N5B	O4A	2.24	3.076	163
—	N8A	O1B	2.03	2.880	171
<sup>a</sup>	N8B	O1A	2.04	2.880	166

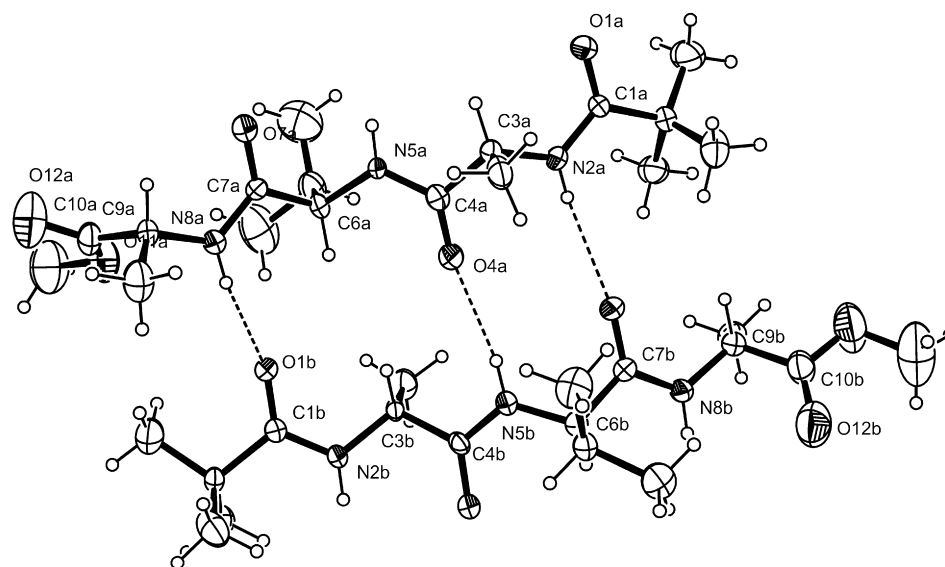
<sup>a</sup> Symmetry equivalents *x*,  $-1+y$ , *z*.

<sup>b</sup> Symmetry equivalents *x*,  $1+y$ , *z*.



**Figure 10.** Crystal packing diagram of peptide **6** showing the intermolecular hydrogen-bonded antiparallel  $\beta$ -sheet structure along crystallographic *b* direction. Hydrogen bonds are shown as dotted lines.

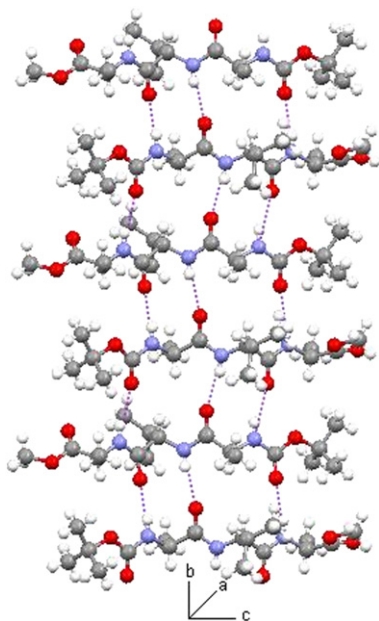
structurally very similar to gelator peptide **1** might in the future help to develop an understanding of why some tripeptides are gelators and some are not.



**Figure 9.** The ORTEP diagram of non-gelator peptide **6** with atomic numbering scheme. Ellipsoids are at the level of 30% probability.

**Table 4.** Characteristics of peptide **6** in molecules A and B and selected torsional angles ( $^{\circ}$ ) for molecules A and B in peptide **6**

Residue	Molecule	$\Phi$	$\varphi$	$\omega$
Ala(1)	A	-145.5	136.0	-175.8
	B	-154.2	152.0	-173.0
Val(2)	A	-134.5	138.7	177.0
	B	-141.6	139.8	178.1
Ala(3)	A	-107.5	-10.4	-179.7
	B	-128.1	173.8	175.0

**Figure 11.** Higher order self-assembly of peptide **6** exhibits complex quaternary  $\beta$ -sheet structure along the screw axis parallel to the crystallographic  $c$  direction. Hydrogen bonds are shown as dotted lines. Non-hydrogen-bonded hydrogen atoms are omitted for clarity. Nitrogen atoms are blue, oxygen atoms are red, and carbon atoms are green.

### 3. Conclusion

This study describes the role of protecting groups in gel formation for the P-AVA-Q (P and Q are the N- and C-terminal protecting groups, respectively) tripeptide series. We made a successful attempt to discuss how small changes in chemical structures either at the N- or C-terminal protecting groups dictate the ability of gel formation in various aromatic organic solvents. These gels formed are characterized by transmission electron microscopy (TEM), FTIR spectroscopy, and wide angle X-ray scattering (WAXS). It has been found that, if we change the C-terminal protecting group from methyl (peptide **8**) to ethyl (peptide **1**) (keeping the N-terminal protecting group same) there is no significant change in the gelation properties. However, variations from ethyl (peptide **1**) to *n*-propyl (peptide **2**) or benzyl ester (peptide **3**) drastically changes the gelation property while the change from ethyl (peptide **1**) to isopropyl (peptide **4**) removes the gelation property. Keeping the same C-terminal group, the results of this gelation study reveal that the change from Boc (*tert*-butoxycarbonyl) (peptide **8**) to the Cbz group (benzyloxycarbonyl) (peptide **7**) does not change the gelation property significantly. Surprisingly, the change from

Boc group to Piv (*tert*-butylcarbonyl group in which deletion of only one oxygen atom occur) (peptide **5**) completely eliminates gelation as indeed does the substitution of the Boc group by an acetyl group (peptide **6**). Some changes in the protecting groups (N- or C-terminal positions) are useful to discover new gelator peptides while some substitutions in the protecting groups are detrimental leading to the removal of the gel-forming tendency. This result may throw some light on the structural features necessary for designing new oligopeptide based gelator molecules in the future. The exact cause of diminishing or/and abolishing of the gelation property of the tripeptide series and the detailed structure–function relationship of gelator versus non-gelator molecules in gel formation are yet to be explored. From the FTIR data of gelator and non-gelator molecules, it has been found that the structures are largely similar ( $\beta$ -sheet structure). However, there are small changes in the supra-molecular structures of gelators and non-gelator molecules, which could cause the difference in properties.

## 4. Experimental

### 4.1. General

The tripeptides were synthesized by conventional solution phase methodology.<sup>19</sup> The Boc/Piv/Cbz/Ac groups were used for N-terminal protection and the C-terminus was protected as a methyl ester, ethyl ester, *n*-propyl ester, benzyl ester, and isopropyl ester. Couplings were mediated by dicyclohexylcarbodiimide–1-hydroxybenzotriazole (DCC–HOBt). The reaction mixture was stirred for three days. The residue was taken in ethyl acetate (60 mL) and the DCU was filtered off. The organic layer was washed with 2 M HCl (3  $\times$  50 mL), brine (2  $\times$  50 mL), 1 M sodium carbonate (3  $\times$  50 mL), and brine (2  $\times$  50 mL), then dried over anhydrous sodium sulfate and evaporated in vacuo. Saponification of methyl esters of dipeptides and tripeptide has been done by 2 M NaOH in methanol and the progress of saponification was monitored by thin layer chromatography (TLC). The reaction mixture was stirred. After 10 h, methanol was removed under vacuum, the residue was taken in 50 mL of water, and washed with diethyl ether (2  $\times$  20 mL). Then the pH of the aqueous layer was adjusted to 2 using 1 M HCl and it was extracted with ethyl acetate (3  $\times$  30 mL). The extracts were pooled, dried over anhydrous sodium sulfate, and evaporated in vacuo to yield as a white solid. All intermediates were characterized by <sup>1</sup>H NMR (300 MHz) and thin layer chromatography (TLC) on silica gel and used without further purification. The final compounds were purified by column chromatography using silica (100–200 mesh) gel as stationary phase and chloroform/methanol as an eluent. The purified final compounds were fully characterized by IR spectroscopy, <sup>1</sup>H NMR spectroscopy, and mass spectrometry.

### 4.2. Syntheses of peptides

**4.2.1. Boc-Ala(1)-OH 9.** See Ref. 20.

**4.2.2. Boc-Ala(1)-Val(2)-OMe 10.** See Ref. 15.

**4.2.3. Boc-Ala(1)-Val(2)-OH 11.** See Ref. 15.

**4.2.4. Boc-Ala(1)-Val(2)-Ala(3)-OEt 1.**  $R_f=0.75$  (CHCl<sub>3</sub>/MeOH=9:1); Yield=2.48 g (6.4 mmol, 80%); mp 106–110 °C; IR (KBr) 3318, 1743, 1696, 1638, 1520 cm<sup>-1</sup>; <sup>1</sup>H NMR (300 MHz, CDCl<sub>3</sub>)  $\delta$  6.75 (d, 1H,  $J=8.1$  Hz); 6.53 (d, 1H,  $J=5.1$  Hz); 4.97 (d, 1H,  $J=5.8$  Hz); 4.54 (m, 1H); 4.27 (m, 1H); 4.23 (m, 1H); 4.11 (m, 2H); 2.20 (m, 1H); 1.45 (s, 9H); 1.41 (d, 3H,  $J=5$  Hz); 1.36 (d, 3H,  $J=6.9$  Hz); 1.30 (t, 3H); 0.95 (m, 6H); <sup>13</sup>C NMR (300 MHz, CDCl<sub>3</sub>)  $\delta$  172.78, 172.49, 170.56, 155.36, 61.19, 58.06, 52.14, 49.98, 47.79, 30.99, 28.11, 18.86, 18.06, 17.79, 13.90; Anal. Calcd for C<sub>18</sub>H<sub>33</sub>N<sub>3</sub>O<sub>6</sub> (387): C, 55.81; N, 10.85; H, 8.53%. Found: C, 55.84; N, 10.83; H, 8.5%;  $[\alpha]_D^{20}$  -78.9 (*c* 1.05, CH<sub>3</sub>OH); MS (ESI)  $m/z$  388.4 (M+H)<sup>+</sup>,  $m/z$  797.5 (2M+Na)<sup>+</sup>.

**4.2.5. Boc-Ala(1)-Val(2)-Ala(3)-O-*n*-Pr 2.**  $R_f=0.65$  (CHCl<sub>3</sub>/MeOH=9:1); Yield=2.45 g (6.1 mmol, 76%); mp 108–113 °C; IR (KBr) 3316, 1739, 1692, 1646, 1530 cm<sup>-1</sup>; <sup>1</sup>H NMR (300 MHz, CDCl<sub>3</sub>)  $\delta$  6.84 (d, 1H,  $J=8.4$  Hz); 6.73 (d, 1H,  $J=6.9$  Hz); 5.09 (d, 1H,  $J=6.9$  Hz); 4.56 (m, 1H); 4.29 (m, 1H); 4.19 (m, 1H); 4.11 (m, 2H); 2.18 (m, 1H); 1.66 (m, 2H); 1.44 (s, 9H); 1.41 (d, 3H,  $J=7.2$  Hz); 1.36 (d, 3H,  $J=7.4$  Hz); 0.96 (m, 6H); 0.92 (m, 3H); <sup>13</sup>C NMR (300 MHz, CDCl<sub>3</sub>)  $\delta$  172.85, 172.69, 170.72, 170.62, 66.92, 58.20, 52.30, 50.16, 48.03, 33.86, 31.06, 28.24, 21.82, 19.05, 18.06, 17.89, 10.20; Anal. Calcd for C<sub>19</sub>H<sub>35</sub>N<sub>3</sub>O<sub>6</sub> (401): C, 56.86; N, 10.47; H, 8.73%. Found: C, 56.88; N, 10.5; H, 8.69%;  $[\alpha]_D^{20}$  -75.0 (*c* 1.05, CH<sub>3</sub>OH); ESI-MS  $m/z$  402.2 (M+H)<sup>+</sup>,  $m/z$  825.5 (2M+Na)<sup>+</sup>.

**4.2.6. Boc-Ala(1)-Val(2)-Ala(3)-OBzl 3.**  $R_f=0.72$  (CHCl<sub>3</sub>/MeOH=9:1); Yield=2.95 g (6.56 mmol, 82%); mp 116–119 °C; IR (KBr) 3301, 1741, 1674, 1642, 1546 cm<sup>-1</sup>; <sup>1</sup>H NMR (300 MHz, CDCl<sub>3</sub>)  $\delta$  7.42–7.32 (5H); 6.83 (d, 1H,  $J=8.4$  Hz); 6.73 (d, 1H,  $J=7.2$  Hz); 6.19 (d, 2H,  $J=6.8$  Hz); 5.06 (d, 1H,  $J=7$  Hz); 4.61 (m, 1H); 4.28 (m, 1H); 4.15 (m, 1H); 2.17 (m, 1H); 1.44 (s, 9H); 1.41 (d, 3H,  $J=7.2$  Hz); 1.36 (d, 3H,  $J=6.9$  Hz); 0.92 (m, 6H); <sup>13</sup>C NMR (300 MHz, CDCl<sub>3</sub>)  $\delta$  172.77, 172.3, 170.59, 135.16, 128.4, 128.22, 126.79, 66.92, 64.98, 58.08, 52.19, 47.93, 33.73, 30.92, 28.12, 24.77, 18.92, 17.94, 17.78; Anal. Calcd for C<sub>23</sub>H<sub>35</sub>N<sub>3</sub>O<sub>6</sub> (449): C, 61.47; N, 9.35; H, 7.8%. Found: C, 61.49; N, 9.36; H, 7.82%;  $[\alpha]_D^{20}$  -69.0 (*c* 1.14, CH<sub>3</sub>OH); ESI-MS  $m/z$  450.4 (M+H)<sup>+</sup>,  $m/z$  921.5 (2M+Na)<sup>+</sup>.

**4.2.7. Boc-Ala(1)-Val(2)-Ala(3)-OMe 8.** See Ref. 15.

**4.2.8. Boc-Ala(1)-Val(2)-Ala(3)-OH 12.** Yield=1.83 g (5.1 mmol, 85%); mp 112–115 °C; IR (KBr) 3321, 1722, 1696, 1642, 1531 cm<sup>-1</sup>; <sup>1</sup>H NMR (300 MHz, (CD<sub>3</sub>)<sub>2</sub>SO)  $\delta$  12.43 (br, 1H); 8.26 (d, 1H,  $J=6.6$  Hz); 7.57 (d, 1H,  $J=8.4$  Hz); 7.05 (d, 1H,  $J=7.5$  Hz); 4.19 (m, 1H); 4.15 (m, 1H); 3.97 (m, 1H); 1.94 (m, 1H); 1.35 (s, 9H); 1.25 (d, 3H,  $J=7.2$  Hz); 1.13 (d, 3H,  $J=7$  Hz); 0.82 (m, 6H); <sup>13</sup>C NMR (300 MHz, CDCl<sub>3</sub>)  $\delta$  177.0, 175.4, 174.7, 157.5, 70.6, 62.8, 54.0, 53.6, 28.7, 28.0, 17.1, 16.3, 16.2; Anal. Calcd for C<sub>16</sub>H<sub>29</sub>N<sub>3</sub>O<sub>6</sub> (359): C, 53.48; N, 11.7; H, 8.01%. Found: C, 53.44; N, 11.73; H, 8.02%.

**4.2.9. Boc-Ala(1)-Val(2)-Ala(3)-*i*-Pr 4.** Boc-Ala(1)-Val(2)-Ala-OH 12 (1.62 g, 4.5 mmol) in DMF (10 mL)

was cooled in an ice-water bath and isopropanol (0.54 g, 9 mmol) was added. It was then added to the reaction mixture, followed immediately by DCC (0.93 g, 4.5 mmol) and HOBt (0.61 g, 4.5 mmol). The reaction mixture was stirred for three days. The residue was taken up in ethyl acetate (40 mL) and the DCU was filtered off. The organic layer was washed with 2 M HCl (3×40 mL), brine (2×50 mL), 1 M sodium carbonate (3×40 mL), brine (2×40 mL), dried over anhydrous sodium sulfate, and evaporated in vacuo to yield **4** as a white solid. Purification was done by silica gel column (100–200 mesh) using chloroform–methanol as an eluent.

$R_f=0.75$  (CHCl<sub>3</sub>/MeOH=9:1); Yield=1.08 g (2.7 mmol, 60%); mp 110–116 °C; IR (KBr) 3323, 1737, 1694, 1644, 1523 cm<sup>-1</sup>; <sup>1</sup>H NMR (300 MHz, CDCl<sub>3</sub>)  $\delta$  6.71 (d, 1H,  $J=7.1$  Hz); 6.43 (d, 1H,  $J=7.6$  Hz); 4.93 (d, 1H,  $J=5.5$  Hz); 4.48 (m, 1H); 4.26 (m, 1H); 4.17 (m, 1H); 3.49 (m, 1H); 2.17 (m, 1H); 1.45 (s, 9H); 1.39 (d, 3H,  $J=7.2$  Hz); 1.35 (d, 3H,  $J=6.9$  Hz); 1.24 (d, 6H); 0.95 (m, 6H); <sup>13</sup>C NMR (300 MHz, CDCl<sub>3</sub>)  $\delta$  172.77, 172.14, 170.45, 69.16, 58.32, 49.44, 48.27, 33.96, 33.24, 30.98, 28.31, 25.63, 24.96, 24.83, 21.71, 19.17, 18.17, 18.12, 17.78; Anal. Calcd for C<sub>19</sub>H<sub>35</sub>N<sub>3</sub>O<sub>6</sub> (401): C, 56.86; N, 10.47; H, 8.73%. Found: C, 56.86; N, 10.48; H, 8.7%;  $[\alpha]_D^{20}$  -47.1 (*c* 1.02, CH<sub>3</sub>OH); ESI-MS  $m/z$  424.2 (M+Na)<sup>+</sup>,  $m/z$  825.5 (2M+Na)<sup>+</sup>.

**4.2.10. Ac-Ala(1)-Val(2)-Ala(3)-OMe 5.** Boc-Ala(1)-Val(2)-Ala-OMe 11 (2.24 g, 6 mmol) was taken and trifluoroacetic (5 mL) acid was added, and the removal of Boc group monitored by TLC. After 2 h, trifluoroacetic acid was removed under vacuum. The residue was taken in water (20 mL) and washed with diethyl ether (2×30 mL). The pH of the aqueous solution was then adjusted to 8 with aq NH<sub>3</sub>. The aqueous portion was evaporated and acetic anhydride (0.5 mL) was added followed by triethylamine (0.7 mL) with continuous stirring. The final compounds were evaporated in vacuo to yield peptide **5** as a white solid.

$R_f=0.55$  (CHCl<sub>3</sub>/MeOH=9:1); Yield=1.32 g (4.2 mmol, 70%); mp 102–106 °C; IR (KBr) 3285, 1744, 1632, 1550 cm<sup>-1</sup>; <sup>1</sup>H NMR (300 MHz, CDCl<sub>3</sub>+20% (CD<sub>3</sub>)<sub>2</sub>SO)  $\delta$  8.43 (d, 1H,  $J=9.8$  Hz); 7.71 (d, 1H,  $J=6.9$  Hz); 7.46 (d, 1H,  $J=9.8$  Hz); 4.48 (m, 1H); 4.42 (m, 1H); 4.29 (m, 1H); 3.73 (s, 3H); 2.18 (m, 1H); 1.99 (s, 3H); 1.41 (d, 3H,  $J=6.6$  Hz); 1.35 (d, 3H,  $J=7.2$  Hz); 0.95 (m, 6H); <sup>13</sup>C NMR (300 MHz, CDCl<sub>3</sub>+20% (CD<sub>3</sub>)<sub>2</sub>SO)  $\delta$  178.92, 175.35, 174.49, 172.55, 63.31, 53.52, 52.77, 35.64, 34.19, 24.19, 23.26, 22.73, 22.35, 13.52; Anal. Calcd for C<sub>14</sub>H<sub>25</sub>N<sub>3</sub>O<sub>5</sub> (315): C, 53.33; N, 13.33; H, 7.94%. Found: C, 53.31; N, 13.35; H, 7.96%;  $[\alpha]_D^{20}$  -77 (*c* 0.8, CH<sub>3</sub>OH); ESI-MS  $m/z$  316.1 (M+H)<sup>+</sup>,  $m/z$  653.3 (2M+Na)<sup>+</sup>.

**4.2.11. Piv-Ala(1)-OH 13.** A solution of alanine (1.34 g, 15 mmol) in a mixture of methanol (15 mL) and 1 M NaOH (15 mL) was stirred and cooled in an ice-water bath. Pivaloyl chloride (1.6 mL, 15 mmol) was added and stirring was continued at room temperature for 6 h. Then the solution was concentrated in vacuo to about 40–60 mL, cooled in an ice-water bath, covered with a layer of ethyl acetate (about 50 mL), and acidified with a dilute solution of KHSO<sub>4</sub> to pH 2–3 (Congo red). The aqueous phase



was extracted with ethyl acetate and this operation was done repeatedly. The ethyl acetate extracts were pooled, washed with water, dried over anhydrous  $\text{Na}_2\text{SO}_4$ , and evaporated in vacuo. Pure material was obtained as a white solid.

Yield=2.39 g (13.8 mmol, 92%); mp 122–126 °C; IR (KBr) 3319, 1726, 1692, 1528  $\text{cm}^{-1}$ ;  $^1\text{H}$  NMR (300 MHz,  $(\text{CD}_3)_2\text{SO}$ )  $\delta$  10.18 (br, 1H); 5.23 (d, 1H,  $J=8.4$  Hz); 4.64 (m, 1H); 1.43 (d, 3H,  $J=7$  Hz); 1.24 (s, 9H);  $^{13}\text{C}$  NMR (300 MHz,  $\text{CDCl}_3$ )  $\delta$  184.4, 177.0, 54.6, 40.8, 25.1, 16.3; Anal. Calcd for  $\text{C}_8\text{H}_{15}\text{NO}_3$  (173): C, 55.49; N, 8.09; H, 4.76%. Found: C, 55.53; N, 8.1; H, 4.72%.

**4.2.12. Piv-Ala(1)-Val(2)-OMe 14.** Yield=2.97 g (10.4 mmol, 80%); mp 113–117 °C; IR (KBr) 3309, 1631, 1542, 1521  $\text{cm}^{-1}$ ;  $^1\text{H}$  NMR (300 MHz,  $\text{CDCl}_3$ )  $\delta$  6.87 (d, 1H,  $J=8.4$  Hz); 6.24 (d, 1H,  $J=6.6$  Hz); 4.57 (m, 1H); 4.48 (m, 1H); 3.74 (s, 3H); 2.20 (m, 1H); 1.37 (d, 3H,  $J=7$  Hz); 1.21 (s, 9H); 0.92 (m, 6H);  $^{13}\text{C}$  NMR (300 MHz,  $\text{CDCl}_3$ )  $\delta$  184.4, 175.4, 172.0, 61.8, 53.1, 50.4, 40.4, 27.4, 25.1, 17.2, 16.6; Anal. Calcd for  $\text{C}_{14}\text{H}_{26}\text{N}_2\text{O}_4$  (286): C, 58.74; N, 9.79; H, 9.09%. Found: C, 58.75; N, 9.82; H, 9.07%.

**4.2.13. Piv-Ala(1)-Val(2)-OH 15.** Yield=2.31 g (8.5 mmol, 85%); mp 124–128 °C; IR (KBr) 3298, 1724, 1628, 1544  $\text{cm}^{-1}$ ;  $^1\text{H}$  NMR (300 MHz,  $(\text{CD}_3)_2\text{SO}$ )  $\delta$  12.56 (br, 1H); 7.64 (d, 1H,  $J=8.4$  Hz); 7.45 (d, 1H,  $J=7.5$  Hz); 4.36 (m, 1H); 4.11 (m, 1H); 2.07 (m, 1H); 1.23 (d, 3H,  $J=10.8$  Hz); 1.09 (s, 9H); 0.84 (m, 6H);  $^{13}\text{C}$  NMR (300 MHz,  $\text{CDCl}_3$ )  $\delta$  184.7, 177.0, 175.4, 64.3, 53.1, 40.4, 27.1, 25.1, 17.2, 16.6; Anal. Calcd for  $\text{C}_{13}\text{H}_{24}\text{N}_2\text{O}_4$  (272): C, 57.35; N, 10.29; H, 8.82%. Found: C, 57.36; N, 10.32; H, 8.84%.

**4.2.14. Piv-Ala(1)-Val(2)-Ala(3)-OMe 6.**  $R_f=0.68$  ( $\text{CHCl}_3/\text{MeOH}=9:1$ ); Yield=2.34 g (6.56 mmol, 82%); mp 105–109 °C; IR (KBr) 3296, 1634, 1546, 1520  $\text{cm}^{-1}$ ;  $^1\text{H}$  NMR (300 MHz,  $\text{CDCl}_3$ )  $\delta$  6.83 (d, 1H,  $J=8.4$  Hz); 6.49 (d, 1H,  $J=7.2$  Hz); 6.16 (d, 1H,  $J=6.6$  Hz); 4.57 (m, 1H); 4.50 (m, 1H); 4.26 (m, 1H); 3.75 (s, 3H); 2.19 (m, 1H); 1.42 (d, 3H,  $J=7.3$  Hz); 1.39 (d, 3H,  $J=7$  Hz); 1.21 (s, 9H); 0.93 (m, 6H);  $^{13}\text{C}$  NMR (300 MHz,  $\text{CDCl}_3$ )  $\delta$  178.39, 173.02, 172.72, 170.68, 58.16, 52.14, 48.41, 47.78, 38.39, 30.93, 27.22, 18.99, 18.86, 17.94, 17.76; Anal. Calcd for  $\text{C}_{17}\text{H}_{31}\text{N}_3\text{O}_5$  (357): C, 57.14; N, 11.76; H, 8.68%. Found: C, 57.17; N, 11.79; H, 8.69%;  $[\alpha]_D^{20} -70.5$  (*c* 1.11,  $\text{CH}_3\text{OH}$ ); ESI-MS  $m/z$  358.3 (M+H) $^+$ ,  $m/z$  737.5 (2M+Na) $^+$ .

**4.2.15. Cbz-Ala(1)-OH 16.** To a solution of alanine (1.34 g, 15 mmol) in water (15 mL), 5 M NaOH (3 mL) was added, stirred, and cooled in an ice-water bath. Benzyl chloroformate in toluene (4.74 mL, 30 mmol) and 2 M NaOH (8 mL) were added slowly in several portions and stirring was continued while the temperature was maintained at about 10 °C. The additions were complete in about one and a half hours. After continued stirring at room temperature for 30 min, the alkalinity of the mixture was adjusted to about pH 10 and the solution was extracted with ether (2 $\times$ 50 mL) and acidified to pH 3 with concentrated HCl. The product separates as oil, which soon solidifies. After several hours in the refrigerator, the disintegrated material

was collected on a filter, washed with water, and dried at 50 °C in vacuo.

Yield=2.88 g (12.9 mmol, 86%); mp 126–130 °C; IR (KBr) 3296, 1724, 1641, 1523  $\text{cm}^{-1}$ ;  $^1\text{H}$  NMR (300 MHz,  $(\text{CD}_3)_2\text{SO}$ )  $\delta$  10.34 (br, 1H); 7.19 (s, 5H); 5.34 (m, 2H); 5.28(d, 1H,  $J=8.4$  Hz); 4.64 (m, 1H); 1.43 (d, 3H,  $J=7$  Hz);  $^{13}\text{C}$  NMR (300 MHz,  $\text{CDCl}_3$ )  $\delta$  177.0, 157.5, 140.9, 128.7, 127.4, 127.3, 69.6, 55.5, 16.2; Anal. Calcd for  $\text{C}_{11}\text{H}_{13}\text{NO}_4$  (223): C, 59.19; N, 6.28; H, 5.83%. Found: C, 59.21; N, 6.33; H, 5.84%.

**4.2.16. Cbz-Ala(1)-Val(2)-OMe 17.** Yield=3.57 g (10.62 mmol, 83%); mp 113–117 °C; IR (KBr) 3297, 1738, 1678, 1521  $\text{cm}^{-1}$ ;  $^1\text{H}$  NMR (300 MHz,  $\text{CDCl}_3$ )  $\delta$  7.36–7.32 (5H); 6.54 (d, 1H,  $J=6.9$  Hz); 5.36 (d, 1H,  $J=6.3$  Hz); 5.12 (s, 2H); 4.52 (m, 1H); 4.27 (m, 1H); 3.74 (s, 3H); 2.16 (m, 1H); 1.39 (d, 3H,  $J=7.2$  Hz); 0.88 (m, 6H);  $^{13}\text{C}$  NMR (300 MHz,  $\text{CDCl}_3$ )  $\delta$  175.4, 172.0, 157.5, 140.9, 128.7, 127.4, 127.3, 69.6, 61.8, 54.4, 54.0, 27.4, 17.1, 16.6; Anal. Calcd for  $\text{C}_{17}\text{H}_{24}\text{N}_2\text{O}_5$  (336): C, 60.71; N, 8.33; H, 7.14%. Found: C, 60.73; N, 8.36; H, 7.15%.

**4.2.17. Cbz-Ala(1)-Val(2)-OH 18.** Yield=2.74 g (8.5 mmol, 85%); mp 127–131 °C; IR (KBr) 3302, 1721, 1638, 528  $\text{cm}^{-1}$ ;  $^1\text{H}$  NMR (300 MHz,  $(\text{CD}_3)_2\text{SO}$ )  $\delta$  12.56 (br, 1H); 7.85 (d, 1H,  $J=8.7$  Hz); 7.45 (d, 1H,  $J=7.8$  Hz); 7.39–7.31 (5H); 5.01 (s, 2H); 4.17 (m, 1H); 4.01 (m, 1H); 2.06 (m, 1H); 1.20 (d, 3H,  $J=7.1$  Hz); 0.87 (m, 6H);  $^{13}\text{C}$  NMR (300 MHz,  $\text{CDCl}_3$ )  $\delta$  177.0, 175.4, 157.5, 140.9, 128.7, 127.4, 127.3, 69.6, 64.3, 54.0, 27.3, 17.1, 16.6; Anal. Calcd for  $\text{C}_{16}\text{H}_{22}\text{N}_2\text{O}_5$  (322): C, 59.63; N, 8.7; H, 6.83%. Found: C, 59.64; N, 8.72; H, 6.86%.

**4.2.18. Cbz-Ala(1)-Val(2)-Ala(3)-OMe 7.**  $R_f=0.72$  ( $\text{CHCl}_3/\text{MeOH}=9:1$ ); Yield=2.8 g (6.88 mmol, 86%); mp 104–108 °C; IR (KBr) 3296, 1740, 1689, 1640, 1534  $\text{cm}^{-1}$ ;  $^1\text{H}$  NMR (300 MHz,  $\text{CDCl}_3$ )  $\delta$  7.38–7.26 (5H); 6.78 (d, 1H,  $J=8.3$  Hz); 6.67 (d, 1H,  $J=6.5$  Hz); 5.48 (d, 1H,  $J=6.7$  Hz); 5.11 (s, 2H); 4.55 (m, 1H); 4.30 (m, 1H); 4.10 (m, 1H); 3.74 (s, 3H); 2.15 (m, 1H); 1.4 (d, 3H,  $J=7.2$  Hz); 1.37 (d, 3H,  $J=7.1$  Hz); 0.93 (m, 6H);  $^{13}\text{C}$  NMR (300 MHz,  $\text{CDCl}_3+30\%$   $(\text{CD}_3)_2\text{SO}$ )  $\delta$  177.64, 177.28, 175.66, 160.61, 141.43, 133.07, 132.57, 70.78, 62.11, 56.56, 55.50, 52.48, 38.47, 35.99, 30.31, 29.51, 23.87, 23.13, 22.58, 21.89; Anal. Calcd for  $\text{C}_{20}\text{H}_{29}\text{N}_3\text{O}_6$  (407): C, 58.97; N, 10.32; H, 7.13%. Found: C, 58.94; N, 10.31; H, 7.14%;  $[\alpha]_D^{20} -55.5$  (*c* 1.0,  $\text{CH}_3\text{OH}$ ); ESI-MS  $m/z$  408.1 (M+H) $^+$ ,  $m/z$  430.1 (M+Na) $^+$ .

### 4.3. Gel melting temperatures

A sealed test tube containing the gel was immersed in a thermostatted oil bath. The temperature was increased at a rate of 2 °C  $\text{min}^{-1}$ . The melting temperatures of the resultant ( $T_{\text{gel}}$ ) were determined by the dropping ball method. The diameter of the ball was 0.6 cm and density of its material was 7.84  $\text{g cm}^{-3}$ .

### 4.4. Transmission electron microscopic studies

Transmission electron microscopy measurements were carried out to observe finer morphological details. A piece of

gel of the corresponding compounds was added onto carbon-coated copper grids (200 mesh) and allowed to dry under vacuum at room temperature for two days. Images were taken at an accelerating voltage of 200 kV. TEM was performed using a JEM 2010 Jeol electron microscope.

#### 4.5. FTIR studies

The FTIR spectra were obtained using a Shimadzu (Japan) model FTIR spectrophotometer. Solvent (toluene) spectra were obtained using a cuvette with 1 mm path length. A Nicolet FTIR instrument (Magna IR-750 spectrometer (series II)) was used to obtain the solid state and gel state FTIR spectra. The solvent spectrum was subtracted from the gel spectrum to obtain tripeptide spectra in the gel state. For the solid state measurements the KBr disk technique was used.

#### 4.6. Mass spectrometry

Mass spectra were recorded on a Micromass Qtof Micro YA263 mass spectrometer by positive mode electrospray ionization.

#### 4.7. Wide angle X-ray diffraction study (WAXS)

The WAXS patterns were made on the tripeptide gels of peptide **1** in toluene, peptide **3** in chlorobenzene, peptide **7** in toluene, dried gel of peptide **1** (5 wt % in toluene), dried gel of peptide **3** (10% in chlorobenzene), dried gel of peptide **7** (5 wt % in toluene), and bulk solids of peptides **1**, **3**, **7**, and **8**. These experiments were carried out in a Seifert X-ray diffractometer (C 3000) with parallel beam optics attachment. The instrument was operated at a 35 kV voltage and 30 mA current and was calibrated with a standard silicon sample. The sample was scanned from 2° to 50° 2θ at the step scan mode (step size 0.03°, present time 2 s) and the diffraction pattern was recorded using a scintillation scan detector.

#### 4.8. Single crystal X-ray diffraction study for peptide 6

C<sub>17</sub>H<sub>31</sub>N<sub>3</sub>O<sub>5</sub>,  $M_w=357.45$ , triclinic, space group *P1*,  $a=9.508(13)$ ,  $b=9.842(13)$ ,  $c=12.404(15)$  Å,  $\alpha=75.92(1)^\circ$ ,  $\beta=74.72(1)^\circ$ ,  $\gamma=72.36(1)^\circ$ ,  $U=1049.74$  Å<sup>3</sup>,  $Z=2$ ,  $D_{\text{calc}}=1.131$  g cm<sup>-3</sup>. Intensity data were collected with Mo Kα radiation using the MARresearch Image Plate System. The crystal was positioned at 70 mm from the Image Plate. One hundred frames were measured at 2° intervals at a counting time of 5 min to give 618 independent reflections. Data analysis was carried out with the XDS program.<sup>21</sup> The structure was solved using direct methods with the Shelx86 program.<sup>22</sup> The non-hydrogen atoms were refined with anisotropic thermal parameters. The hydrogen atoms were included in geometric positions and given thermal parameters equivalent to 1.2 times those of the atom to which they were attached. The structure was refined on  $F^2$  using Shelxl.<sup>23</sup> The final *R* values were *R*1 0.0559 and *wR*2 0.1043 for 3521 data with  $I>2\sigma(I)$ . The largest peak and hole in the final difference Fourier were 0.272 and -0.136 eÅ<sup>-3</sup>. The data have been deposited at the Cambridge Crystallographic Data Center with reference number CCDC 289554.

#### Acknowledgements

This research is supported by a grant from Department of Science and Technology (DST), India (Project no. SR/S5/OC-29/2003). We thank EPSRC and the University of Reading, UK for funds for the Image Plate System. A.K.D. and P.P.B. wish to acknowledge the CSIR, New Delhi, India for financial assistance. We gratefully acknowledge the Nanoscience and technology initiative of Department of Science and Technology of Govt. of India, New Delhi for using TEM facility.

#### References and notes

- (a) Terech, P.; Weiss, R. G. *Chem. Rev.* **1997**, *97*, 3133–3160; (b) van Esch, J.; Feringa, B. L. *Angew. Chem., Int. Ed.* **2000**, *39*, 2263–2266; (c) Abdallah, D. J.; Weiss, R. G. *Adv. Mater.* **2000**, *12*, 1237–1247; (d) Sangeetha, N. M.; Maitra, U. *Chem. Soc. Rev.* **2005**, *34*, 821–836; (e) George, M.; Weiss, R. G. *Acc. Chem. Res.* **2006**, *39*, 489–497.
- (a) Gao, P.; Zhan, C.; Liu, L.; Zhou, Y.; Liu, M. *Chem. Commun.* **2004**, 1174–1175; (b) Suzuki, M.; Nakajima, Y.; Yumoto, M.; Kimura, M.; Shirai, H.; Hanabusa, K. *Org. Biomol. Chem.* **2004**, *2*, 1155–1159; (c) Suzuki, M.; Sato, T.; Kurose, A.; Shirai, H.; Hanabusa, K. *Tetrahedron Lett.* **2005**, *46*, 2741–2745.
- George, S. J.; Ajayaghosh, A. *Chem.—Eur. J.* **2005**, *11*, 3217–3227.
- (a) Zubarev, E. R.; Pralle, M. U.; Sone, E. D.; Stupp, S. I. *J. Am. Chem. Soc.* **2001**, *123*, 4105–4106; (b) Tew, G. N.; Pralle, M. U.; Stupp, S. I. *J. Am. Chem. Soc.* **1999**, *121*, 9852–9866.
- (a) Zhan, C.; Gao, P.; Liu, M. *Chem. Commun.* **2005**, 462–464; (b) Díaz, N.; Simon, F.-X.; Schmutz, M.; Rawiso, M.; Decher, G.; Jestin, J.; Mésini, P. J. *Angew. Chem., Int. Ed.* **2005**, *44*, 3260–3264; (c) Chen, J.; Xue, C.; Ramasubramaniam, R.; Liu, H. *Carbon* **2006**, *44*, 2142–2146.
- (a) Sone, E. D.; Zubarev, E. R.; Stupp, S. I. *Angew. Chem., Int. Ed.* **2002**, *41*, 1705–1709; (b) Zhan, C.; Wang, J.; Yuan, J.; Gong, H.; Liu, Y.; Liu, M. *Langmuir* **2003**, *19*, 9440–9445; (c) Jung, J. H.; Kobayashi, H.; Masuda, M.; Shimizu, T.; Shinkai, S. *J. Am. Chem. Soc.* **2001**, *123*, 8785–8789; (d) van Bommel, K. J. C.; Friggeri, A.; Shinkai, S. *Angew. Chem., Int. Ed.* **2003**, *42*, 980–999; (e) Llusar, M.; Roux, C.; Pozzo, J. L.; Sanchez, C. *J. Mater. Chem.* **2003**, *13*, 442–444; (f) Wei, Q.; James, S. L. *Chem. Commun.* **2005**, 1555–1556; (g) Xue, P.; Lu, R.; Li, D.; Jin, M.; Tan, C.; Bao, C.; Wang, Z.; Zhao, Y. *Langmuir* **2004**, *20*, 11234–11239; (h) Xue, P.; Lu, R.; Huang, Y.; Tan, C.; Bao, C.; Wang, Z.; Zhao, Y. *Langmuir* **2004**, *20*, 6470–6475; (i) Hanabusa, K.; Numazawa, T.; Kobayashi, S.; Suzuki, M.; Shirai, H. *Macromol. Symp.* **2006**, *235*, 52–56.
- (a) Friggeri, A.; Gronwald, O.; van Bommel, K. J. C.; Shinkai, S.; Reinhoudt, D. N. *J. Am. Chem. Soc.* **2002**, *124*, 10754–10758; (b) Shumburo, A.; Biewer, M. C. *Chem. Mater.* **2002**, *14*, 3745–3750; (c) George, M.; Snyder, S. L.; Terech, P.; Glinka, C. L.; Weiss, R. G. *J. Am. Chem. Soc.* **2003**, *125*, 10275–10283; (d) Ryu, S. Y.; Kim, S.; Seo, J.; Kim, Y.-W.; Kwon, O.-H.; Jang, D.-J.; Park, S. Y. *Chem. Commun.* **2004**, 70–71; (e) An, B.-K.; Lee, D.-S.; Park, Y.-S.; Song, H.-S.; Park, S. Y. *J. Am. Chem. Soc.* **2004**, *126*, 10232–10233.
- (a) Jung, J. H.; Shinakai, S.; Shimizu, T. *Nano Lett.* **2002**, *2*, 17–20; (b) Kobayashi, S.; Hamasaki, N.; Suzuki, M.; Kimura, M.;

- Shinkai, H.; Hanabusa, K. *J. Am. Chem. Soc.* **2002**, *124*, 6550–6551; (c) Yang, Y.; Suzuki, M.; Shirai, H.; Kurose, A.; Hanabusa, K. *Chem. Commun.* **2005**, 2032–2034; (d) Jung, J. H.; Kobayashi, H.; van Bommel, K. J. C.; Shinkai, S.; Shimizu, T. *Chem. Mater.* **2002**, *14*, 1445–1447; (e) Kanie, K.; Sugimoto, T. *Chem. Commun.* **2004**, 1584–1585; (f) Suzuki, M.; Nakajima, Y.; Sato, T.; Shirai, H.; Hanabusa, K. *Chem. Commun.* **2006**, 377–379.
9. Kiyonaka, S.; Shinkai, S.; Hamachi, I. *Chem.—Eur. J.* **2003**, *9*, 976–983.
10. Wang, G.; Hamilton, A. D. *Chem.—Eur. J.* **2002**, *8*, 1954–1961.
11. Wang, G.; Hamilton, A. D. *Chem. Commun.* **2003**, 310–311.
12. Kisiday, J.; Jin, M.; Kurz, B.; Hung, H.; Semino, C.; Zhang, S.; Grodzinsky, A. J. *Proc. Natl. Acad. Sci. U.S.A.* **2002**, *99*, 9996–10001.
13. (a) Zhang, Y.; Gu, H.; Yang, Z.; Xu, B. *J. Am. Chem. Soc.* **2003**, *125*, 13680–13681; (b) Pochan, D. J.; Schneider, J. P.; Kretsinger, J.; Ozbas, B.; Rajagopal, K.; Haines, L. *J. Am. Chem. Soc.* **2003**, *125*, 11802–11803; (c) Nowak, A. P.; Breedveld, V.; Pine, D. J.; Deming, T. J. *J. Am. Chem. Soc.* **2003**, *125*, 15666–15670; (d) Schneider, J. P.; Pochan, D. J.; Ozbas, B.; Rajagopal, K.; Pakstis, L.; Kretsinger, J. *J. Am. Chem. Soc.* **2002**, *124*, 15030–15037; (e) Hartgerink, J. D.; Beniash, E.; Stupp, S. I. *Proc. Natl. Acad. Sci. U.S.A.* **2002**, *99*, 5133–5138; (f) Aggelli, A.; Bell, M.; Boden, N.; Keen, J. N.; Knowles, P. F.; McLeish, T. C. B.; Pitkeathly, M.; Radford, S. E. *Nature* **1997**, *386*, 259–262; (g) Kirschner, D. A.; Inouye, H.; Duffy, L. K.; Sinclair, A.; Lind, M.; Selkoe, D. J. *Proc. Natl. Acad. Sci. U.S.A.* **1987**, *84*, 6953–6957.
14. (a) Malik, S.; Maji, S. K.; Banerjee, A.; Nandi, A. K. *J. Chem. Soc., Perkin Trans. 2* **2002**, 1177–1186; (b) Maji, S. K.; Malik, S.; Drew, M. G. B.; Nandi, A. K.; Banerjee, A. *Tetrahedron Lett.* **2003**, *44*, 4103–4107; (c) Jayakumar, R.; Murugesan, M.; Asokan, C.; Scibioh, M. A. *Langmuir* **2000**, *16*, 1489–1496; (d) Ganesh, S.; Prakash, S.; Jayakumar, R. *Biopolymers* **2003**, *70*, 346–354; (e) Hanabusa, K.; Naka, Y.; Koyama, T.; Shirai, H. *J. Chem. Soc., Chem. Commun.* **1994**, 2683–2684.
15. (a) Das, A. K.; Manna, S.; Drew, M. G. B.; Malik, S.; Nandi, A. K.; Banerjee, A. *Supramol. Chem.* **2006**, *18*, 455–464; (b) Das, A. K.; Banerjee, A. *Macromol. Symp.* **2006**, *241*, 14–22.
16. van Esch, J.; Schoonbeek, F.; de Loos, M.; Kooijman, H.; Spek, A. L.; Kellogg, R. M.; Feringa, B. L. *Chem.—Eur. J.* **1999**, *5*, 937–950.
17. Moretto, V.; Crisma, M.; Bonora, G. M.; Toniolo, C.; Balam, H.; Balam, P. *Macromolecules* **1989**, *22*, 2939–2944.
18. Ramachandran, G. N.; Sasisekharan, V. *Adv. Protein Chem.* **1968**, *23*, 284–438.
19. Bodanszky, M.; Bodanszky, A. *The Practice of Peptide Synthesis*; Springer: New York, NY, 1984; pp 1–282.
20. Maji, S. K.; Haldar, D.; Drew, M. G. B.; Banerjee, A.; Das, A. K.; Banerjee, A. *Tetrahedron* **2004**, *60*, 3251–3259.
21. Kabsh, W. J. *Appl. Crystallogr.* **1988**, *21*, 916–932.
22. Sheldrick, G. M. *Acta Crystallogr., Sect. A: Fundam. Crystallogr.* **1990**, *46*, 467–473.
23. Sheldrick, G. M. *Program for Crystal Structure Refinement*; University of Göttingen: Germany, 1997.